Revista Chilena de Historia Natural
77: 87-105, 2004

Bio-optical characteristics of phytoplankton populations in the upwelling system off the coast of Chile

Características (bio-ópticas) de poblaciones de fitoplancton en el sistema de surgencia de la costa de Chile

VENETIA STUART[1,2,*], OSVALDO ULLOA[3,4], GADIEL ALARCÓN[3], SHUBHA SATHYENDRANATH[1,2], HEATHER MAJOR[2], ERICA J.H. HEAD[1] & TREVOR PLATT[1]

[1]Biological Oceanography Division, Bedford Institute of Oceanography, Box 1006, Dartmouth, Nova Scotia Canada B2Y 4A2
[2]Department of Oceanography, Dalhousie University, Halifax, Nova Scotia, Canada, B3H 4J1
[3]Programa Regional de Oceanografía Física y Clima (PROFC), Universidad de Concepción, Casilla 160-C, Concepción, Chile
[4]Centro de Investigación Oceanográfica (COPAS) and Departamento de Oceanografía, Universidad de Concepción, Casilla 160-C, Concepción, Chile
*Corresponding author: e-mail: vstuart@dal.ca

ABSTRACT

Phytoplankton samples collected from two cruises off the coast of Chile were analysed for pigment composition and absorption characteristics. High pigment concentrations (up to 20 mg chl-*a* m^{-3}) were found in the upwelled waters over the shelf break off the coast of Concepción during spring (October 1998), but relatively oligotrophic conditions were found further offshore. Similarly, stations further north (between Coquimbo and Iquique), sampled during the austral summer (February 1999), also showed low pigment concentrations, characterised by the presence of prymnesiophytes, and cyanobacteria including *Prochlorococcus* sp. The specific absorption coefficient of phytoplankton at 443 nm ($a^*_{ph}(443)$) was much higher for the offshore population than the inshore population, which was dominated by large diatoms. These differences are attributed to changes in pigment packaging and pigment composition. The relative proportion of non-photosynthetic carotenoids to chl-*a*, together with the ratio of the peak height of the Gaussian bands in the blue and red regions of the spectrum, $p(435)/p(676)$, (an indicator of the importance of the packaging effect) could account for up to 92 % of the total variation in $a^*_{ph}(443)$. Blue/green absorption ratios were strongly related to the relative concentration of 19'-hexanoyloxyfucoxanthin and fucoxanthin. A reasonable agreement was found between in situ and satellite estimates of chl-*a* (SeaWiFS data) despite the large variability in phytoplankton specific absorption coefficients, suggesting that the 'global' absorption-to-chlorophyll relationships encompass the regional variations observed off the coast of Chile. Satellite chl-*a* was overestimated in oligotrophic water when compared to HPLC chl-a measurements, apparently because of the high specific absorption coefficients of phytoplankton in the offshore waters. On the other hand, ship and satellite data were in closer agreement when in situ fluorometric chl-*a* data was used. It is likely that the correlation between in situ and satellite chl-a could be improved by using regional algorithms.

Key words: phytoplankton absorption, HPLC pigments, SeaWiFS ocean-colour, Chile.

RESUMEN

La composición de pigmentos y las características de absorción fueron analizadas en muestras de fitoplancton recolectadas en dos cruceros frente a las costas Chile. Se encontraron altas concentraciones de pigmentos (hasta 20 mg chl-*a* m^{-3}) en aguas de surgencia sobre el quiebre de la plataforma frente a Concepción durante la primavera, octubre de 1998; sin embargo, se encontraron condiciones relativamente oligotróficas costa afuera. De manera similar, estaciones más al norte (entre Coquimbo e Iquique), muestreadas durante el verano austral (febrero de 1999), también mostraron bajas concentraciones de pigmentos, caracterizados por la presencia de primnesioficeas y cianobacterias (*Synechococccus* sp. y *Prochlorococcus* sp.). El coeficiente de absorción específico del fitoplancton a 443 nm ($a^*_{ph}(443)$) fue mucho mayor para las poblaciones costa afuera que para las poblaciones costeras, las cuales estaban dominadas por diatomeas. Esta diferencia fue atribuida a cambios en el empaquetamiento y composición de pigmentos. La proporción relativa entre carotenoides no-fotosintéticos y chl-*a*, junto con la razón de la altura del pico de las bandas Gausianas en las regiones azul y roja del espectro $p(435)/p(676)$ (un índice del efecto de empaquetamiento), representa hasta el 92 % de la variación total en $a^*_{ph}(443)$. Las razones de absorción azul/verde estuvieron relacionadas fuertemente a la concentración relativa de 19'-hexanoiloxifucoxantina y fucoxantina. Se encontró una relación aceptable entre

las estimaciones de chl-*a* (datos de SeaWiFS) medidas in situ y las obtenidas con el satélite, a pesar de la gran variabilidad en los coeficientes de absorción específica del fitoplancton, sugiriendo que las relaciones de absorción de clorofila "global" abarcan las variaciones regionales observadas a la altura de las costas de Chile. Las mediciones de chl-*a* satelitales fueron sobreestimadas en aguas oligotróficas cuando se compararon con determinaciones HPLC de chl- *a*, aparentemente por los coeficientes específicos de absorción altos del fitoplancton en mar abierto. Además, los datos obtenidos por barco y de satélite estuvieron estrechamente relacionados cuando se utilizaron datos de chl- *a* in situ y fluorométricos. Probablemente la correlación entre la chl- *a* in situ y satelital podría ser mejorada utilizando algoritmos regionales.

Palabras clave: absorción fitoplanctónica, HPLC pigmentos, SeaWiFS color del océano satelital, Chile.

INTRODUCTION

The Humboldt current system off the coasts of Peru and Chile is one of the major upwelling systems of the world. Dominant along-shore winds induce an offshore transport of surface waters, resulting in the upwelling of cool, nutrient-rich waters into the euphotic layers. This leads to increased phytoplankton production, which in turn supports prolific secondary production of zooplankton, fish, birds and mammals. This extensive coastal upwelling region is extremely important to the economy because it supports one of the most productive fisheries in the world (Ryther, 1969). Upwelling tends to occur year-round off the coast of Peru and northern Chile, but only during the spring (September/October) and summer months (December to March) off the coast of central Chile. Phytoplankton populations in these productive upwelling zones are characterised by rapidly growing, large-celled species such as diatoms (Mackey et al. 1998). In contrast, the waters further offshore are generally less productive and are dominated by smaller phytoplankton species, implying regional differences in phytoplankton distributions off the coast of Chile (Morales et al. 2001).

Systematic variations in the distribution, abundance and pigment composition of phytoplankton assemblages are known to occur over large spatial scales, such as along the Atlantic Meridional Transect between the United Kingdom and Falkland Islands (Gibb et al. 2000). Conversely, changes in phytoplankton composition are also known to occur over relatively small spatial scales, for example between the coast of Labrador and the Greenland Shelf (Lutz et al. 1996, Stuart et al. 2000). These changes in phytoplankton species composition (with accompanying changes in pigment composition) are often accompanied by changes in phytoplankton specific absorption coefficients (light absorption divided by pigment concentration), which exhibit regional, as well as seasonal variations (Bricaud & Stramski 1990, Hoepffner & Sathyendranath 1992, Lutz et al. 1996, Sathyendranath et al. 1999).

Although a considerable literature exists on the absorption and scattering of light by phytoplankton, relatively few studies have been conducted on phytoplankton populations off the coast of Chile. It is important to understand regional variations in phytoplankton specific absorption coefficients, since they constitute a major factor influencing the reflectance signal from seawater. Water-leaving radiance in the visible domain of the electromagnetic spectrum (which is related to reflectance) is used in ocean-colour algorithms to retrieve chlorophyll concentrations from remotely-sensed ocean-colour data (O'Reilly et al. 1998).

The pigment composition of phytoplankton from the coastal upwelling zone off the coast of Chile is examined in detail to characterise the spatial variability and species composition of phytoplankton in this dynamic region. In addition, bio-optical characteristics of the phytoplankton are examined to relate variability in phytoplankton spectral absorption coefficients to pigment composition and pigment packaging. The observed variability in optical characteristics of the phytoplankton bears on the reliability of routine algorithms used to retrieve chlorophyll from remotely-sensed ocean-colour data.

MATERIAL AND METHODS

Data were collected during two cruises off the coast of Chile, onboard the R/V Abate Molina. The Multidisciplinary Intensive Research Cruise (MIRC) was conducted during the spring upwelling period (October 1998) along a transect off the Bay of Concepción (approximately 36º S). The second cruise, the Coquimbo-Iquique cruise, was conducted during the austral summer (February 1999), and sampled the region farther north between Coquimbo and Iquique (20-30º S). Figure 1 shows the location of all sampling stations. The

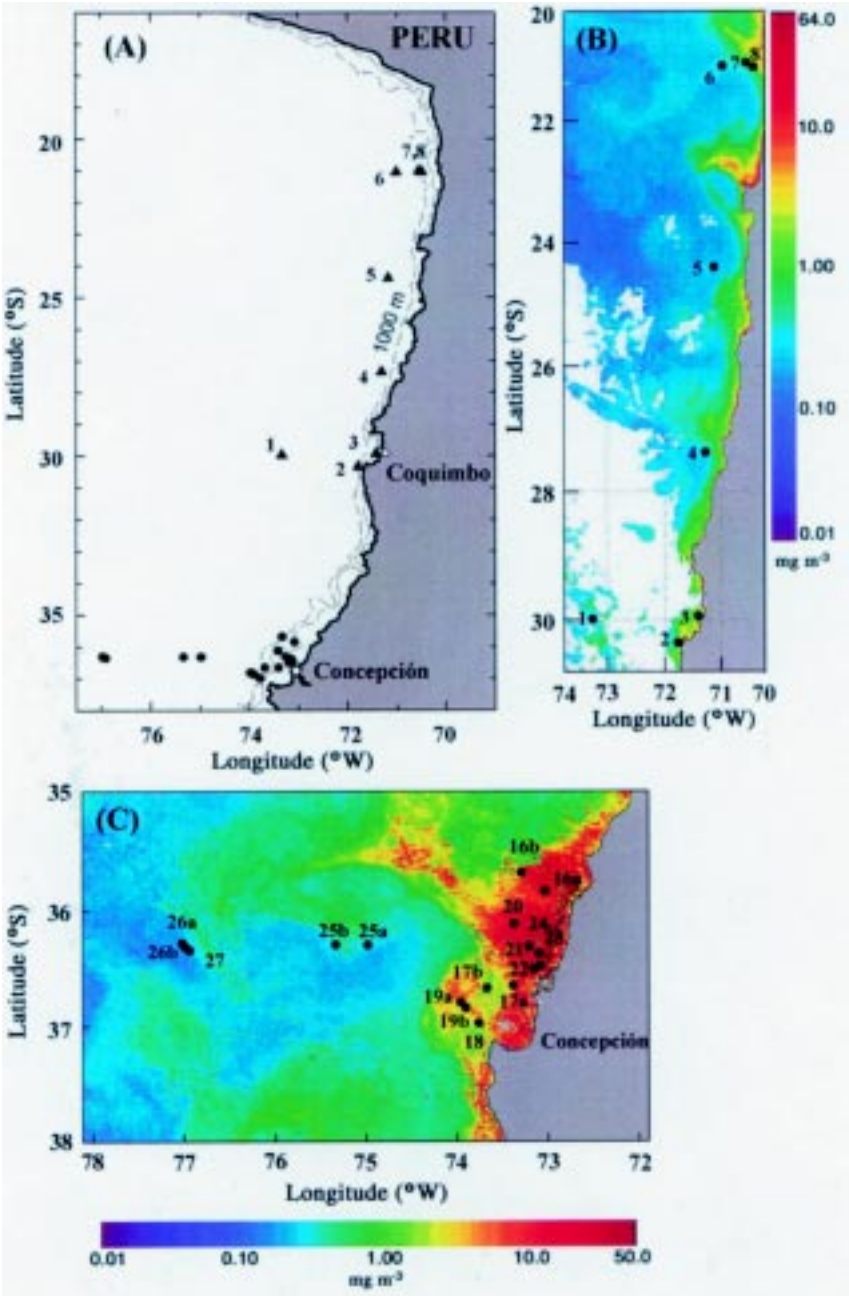

Fig. 1: (A) Map of the study area off the coast of Chile showing the location of sampling stations for the Multidisciplinary Intensive Research Cruise (MIRC), October, 1998 (solid circles), and the Coquimbo-Iquique cruise, February, 1999 (solid triangles). Bathymetric contours at 200 m and 1,000 m are indicated with a dashed line. (B) Composite satellite chl-*a* image (10-16 February, 1999) for the Coquimbo-Iquique cruise. (C) Composite satellite chl-*a* image (16-27 October, 1998) for the area off Concepción showing location of sampling stations for the MIRC cruise. Both satellite images derived from SeaWiFS data using the OC4v4 algorithm.

(A) Mapa del área de estudio frente a la costa de Chile que muestra la ubicación de las estaciones de muestreo del Multidisciplinary Intensive Research Cruise (MIRC), en octubre de 1998 (círculos rellenos), y el crucero Coquimbo-Iquique, en febrero de 1999 (triángulos rellenos). Las isóbatas de 200 y 1.000 m también se indican en ambos mapas. (B) Imagen satelital compuesta de chl- *a* (10 al 16 de febrero de 1999) del crucero Coquimbo-Iquique. (C) Imagen satelital compuesta de chl- *a* (16 al 27 de octubre de 1998) para el área frente a Concepción mostrando la localización de las estaciones de muestreo del crucero MIRC. Ambas imágenes satelitales fueron derivadas del SeaWiFS utilizando el algoritmo OC4v4.

TABLE 1

Sampling dates, station location and range of depths sampled during the MIRC Concepción cruise and the Coquimbo-Iquique cruise, for analysis of HPLC pigment composition, fluorometric pigment analysis and phytoplankton absorption characteristics (sampling intervals ranged from 3 m to 25 m depending upon depth). Satellite-derived chl-*a* concentration (mean of 9 pixels ± SD) for match-up stations (surface samples) and the time difference between the satellite overpass and the time of in situ sampling, is also shown

Fechas de muestreo, ubicación de las estaciones y rango de profundidades muestreadas durante el crucero MIRC frente a Concepción y durante el crucero Coquimbo-Iquique, para el análisis de composición de pigmentos por HPLC, análisis fluorométrico de pigmento y características de absorción del fitoplancton (los intervalos de muestreo variaron entre 3 m a 25 m, dependiendo de la profundidad). También se muestra la concentración de chl-*a* derivada del satélite (media de 9 pixeles ± DE) para las estaciones coincidentes (muestras superficiales) y la diferencia temporal entre el paso del satélite y el tiempo de muestreo in situ

Cruise	Date	Station	Latitude (ºS)	Longitude (ºW)	Sampling depth (m)	Number of samples	Satellite chlorophyll (± SD)	Time difference (h:min)
MIRC	16/10/98	16a	35.86	73.07	0-17	3	-	-
	16/10/98	16b	35.70	73.33	0-12	2	-	-
	17/10/98	17a	36.67	73.40	0	1	2.65 ± 0.26	6:43
	17/10/98	17b	36.70	73.68	0-25	5	2.13 ± 0.28	2:23
	18/10/98	18	37.03	73.77	0-50	9	4.20 ± 1.23	4:52
	19/10/98	19	36.87	73.92	0-100	11	-	-
	19/10/98	19b	36.83	73.97	0	1	-	-
	20/10/98	20	36.14	73.41	0-100	11	19.72 ± 7.66	6:05
	21/10/98	21	36.50	73.12	0-75	11	6.37 ± 0.70	4:14
	22/10/98	22	36.52	73.18	0-50	9	10.93 ± 2.84	5:38
	23/10/98	23	36.40	73.14	0-25	6	20.91 ± 5.1	4:50
	24/10/98	24	36.33	73.24	0-25	7	-	-
	25/10/98	25a	36.33	74.97	0	1	0.27 ± 0.02	3.51
	25/10/98	25b	36.33	75.32	0-60	7	0.42 ± 0.05	1:11
	26/10/98	26a	36.33	76.95	0-75	9	0.36 ± 0.09	4:49
	26/10/98	26b	36.32	76.96	0	1	0.18 ± 0.01	3:09
	27/10/98	27	36.35	76.92	0-60	9	-	-
Coquimbo-	10/2/99	1	29.99	73.33	0	1	-	-
Iquique	11/2/99	2	30.36	71.77	0	1	-	-
	12/2/99	3	29.94	71.41	0	1	-	-
	13/2/99	4	27.36	71.30	0	1	-	-
	14/2/99	5	24.39	71.16	0	1	-	-
	15/2/99	6	21.07	71.00	0	1	-	-
	16/2/99	7	21.07	70.48	0-50	6	-	-
	16/2/99	8	21/02	70.54	0-80	4	-	-

total number of samples collected at each station for the analysis of pigment content and phytoplankton absorption characteristics is given in Table 1 (note: stations for the MIRC cruise have been numbered according to sampling date).

For the determination of pigment content and phytoplankton absorption characteristics, samples from discrete depths were collected from Niskin bottles mounted on a rosette with an integrated CTD system (Seabird Model SBE 25). For fluorometric pigment determination, triplicate 100 mL water samples were filtered onto 25 mm GF/F glass fibre filters at a vacuum differential of < 200 mm Hg, and kept frozen in liquid nitrogen, until processed in the laboratory. Samples were extracted overnight in 10 mL 90 % acetone at -20 ºC, and chl-*a* and phaeopigment concentrations were subsequently measured using a Turner Designs fluorometer, according to the method of Holm-Hansen et al. (1965). For high-performance liquid chromatography (HPLC) pigment determinations and measurement of phytoplankton absorption characteristics, duplicate seawater samples (250–1,000 mL depending on phytoplankton concentration) were filtered onto 25 mm GF/F glass fibre filters, and frozen immediately in liquid nitrogen for later analysis in the laboratory.

Pigment analysis

Reverse-phase, high-performance liquid chromatography was used to determine pigment concentrations as described in Head & Horne (1993). Filters were homogenised in 1.5 mL of 90 % acetone, centrifuged and diluted with 0.5 M ammonium acetate buffer at a ratio of 2:1 before injection. The samples were run on a Beckman C18, reverse-phase, 3-µm Ultrasphere column (70 x 4.6 mm), using the solvents methanol:0.5 M ammonium acetate (80:20) and methanol:ethyl acetate (70:30). Chromatographic peaks were detected by a UV-VIS photodiode array detector (Beckman 168) and identified by retention time and comparison of absorbance spectra with spectra of pigments from standard microalgal cultures. In addition, standards of chl-*a*, chl-*b* and b-carotene were obtained from Sigma Chemical Company. Divinyl chl-*a* and divinyl chl-*b* (chl-a_2 and -b_2), characteristic of *Prochlorococcus* sp., were quantified by acidifying samples with 1 N HCL and recording the peak heights of divinyl phaeophytin-like pigments. Note that HPLC determined chl-*a* represents a total of chlorophyllide-*a*, mono- and divinyl chl-*a*, plus the chl-*a* epimer and allomer.

Light absorption by phytoplankton

The optical density of the total particulate material relative to a blank filter was measured from 350-750 nm using a dual-beam Shimadzu UV-2101 PC scanning spectrophotometer equipped with an integrating sphere. A GF/F filter saturated with filtered seawater was used as a blank and scans were run with a 5 nm bandwidth. The detrital component of the total particulate absorption was estimated according to the method of Kishino et al. (1985). After recording the spectra, pigments were extracted from the filters using 20 mL hot methanol (100 %), followed by 20 mL of filtered seawater (to remove any residual solvents). Blank filters were treated in the same manner. The absorption of these extracted filters was then measured as before. A few filters contained non-extracted residual pigments and/or phaeopigments, which may cause an underestimation of phytoplankton absorption. As a correction, the detrital absorption data for these samples were fitted with an exponential curve, as described in Sathyendranath et al. (1999). The absorption coefficient of detrital material at 440 nm was relatively small, representing on average about 12.7 % of total particulate absorption (range 3.3-36.2 % for both cruises). The contribution of detritus to total particulate absorption generally increased with depth.

Optical density measurements were divided by the geometrical path length (volume filtered divided by clearance area of the filter) and multiplied by a factor of 2.3 (conversion factor for transforming decimal logarithms to natural logarithms) to obtain the absorption coefficient. The value of the absorption coefficient at 750 nm was subtracted from the values at all other wavelengths, as a rudimentary correction for errors due to scattering by the phytoplankton cells. Measurements were corrected for path-length amplification due to scattering by the filter, using the ß-correction algorithms of Hoepffner & Sathyendranath (1992, 1993) and Moore et al. (1995), weighted according to phytoplankton species composition as determined by HPLC analysis (see Stuart et al. 1998). Absorption by the phytoplankton component, $a_{ph}(\lambda)$, was then obtained by subtracting the detritus curve, $a_{ph}(\lambda)$, (or the exponential curve) from the total particulate absorption spectrum. Pigment specific absorption coefficients of phytoplankton $a^*_{ph}(\lambda)$ were calculated by dividing absorption by HPLC-determined chl-*a* concentration.

Each phytoplankton absorption spectrum was then decomposed into 13 Gaussian bands representing absorption by the major phytoplankton pigments (chls-*a*, -*b* and -*c*, and carotenoids) as described in detail in Hoepffner & Sathyendranath (1991, 1993). The initial centers and halfwidths (nm) of each Gaussian band were taken from Hoepffner & Sathyendranath (1991, 1993), but the initial peak height of each band ($p(\lambda)$ in m^{-1}) was adjusted according to the magnitude of the absorption at 440 nm. Gaussian bands nominally centered around 384, 413, 435, 623, 676 and 700 nm correspond to absorption by chl-*a*, 464 and 655 nm to absorption by chl-*b*, 461, 583 and 644 nm to absorption by chl-*c* and 490 and 532 nm to absorption by total carotenoids (note: band 583 nm is also related to chl-*a*).

Satellite-derived chl-a

Satellite data from the SeaWiFS ocean-colour sensor for the period 16-27 October, 1998, were obtained from NASA Goddard Space Flight Center, Distributed Active Archive Center (DAAC). Daily satellite images were processed using SeaDAS software (version 4.1), correcting for atmospheric influences and applying default values for various masks (e.g.,

clouds, sunglint, high aerosol optical thickness). Satellite-derived values of chl-*a* (Chl_{sat}) were computed using the default parameter values of the standard OC4v4 algorithm (O'Reilly et al. 2000) in combination with regional near-real-time meteorological data and ozone concentrations. This model estimates in situ chl-*a* from the remote sensing reflectance, $R_{rs}(\lambda)$, at four wavebands, and uses the maximum of three band ratios $R_{rs}(443)/R_{rs}(555)$, $R_{rs}(490)/R_{rs}(555)$, or $R_{rs}(510)/R_{rs}(555)$ in the algorithm (see O'Reilly et al., 1998). Figure 1 shows composite chl-*a* images for each cruise, averaged over the duration of the cruise. It is apparent that, during the Coquimbo-Iquique cruise, most of the sampling stations were located in oligotrophic waters (Fig. 1B) whereas in the MIRC cruise many of the stations occupied were in a dense upwelling plume (Fig. 1C).

RESULTS

Hydrographic conditions

Temperature profiles for selected stations from the MIRC cruise are shown in Fig. 2. Inshore stations (Stations 18-22) were characterised by relatively low surface temperatures (10.8-11.5 ^{o}C), characteristic of an upwelling area. Station 22 exhibited a well-defined mixed layer down to a depth of around 30 m, whereas Stations 20 and 21 exhibited a somewhat shallower mixed-layer (down to ~ 20 m) although this was not well-defined. Further offshore surface temperatures were warmer (13.5 to 14.5 ^{o}C). Station 25b showed some evidence of surface warming, with a deep mixed layer (~70 m), whereas the stations farthest offshore (Stations 26a and 27) displayed a well-mixed layer down to a depth of around 50 m.

Pigment composition along the transect

Figure 3 shows the total HPLC-derived chl-a concentration (chl-a + divinyl chl-a) in all samples collected from the surface layers of the water column (0-5 m), plotted against approximate distance offshore, for both cruises. During the MIRC cruise (spring), high pigment concentrations (up to 20 mg chl-a m^{-3}) were found in the upwelled waters over the shelf break (~ 100 km offshore) which is also apparent in the satellite image (Fig. 1C). Relatively oligotrophic conditions were found further offshore, as has been found in several other studies off the coast of Chile (Thomas et

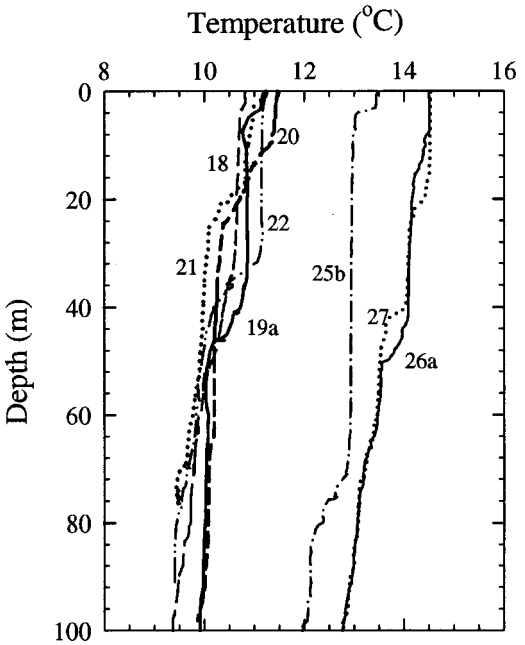

Fig. 2: Temperature-depth profiles for selected stations from the MIRC cruise (October, 1998). Stations 18-22 represent the inshore stations, while Stations 25-27 are located further offshore.

Perfiles de temperatura-profundidad para las estaciones escogidas del crucero MIRC (octubre de 1998). Las estaciones 18-22 representan estaciones costeras, mientras que las estaciones 25-27 están ubicadas más costa afuera.

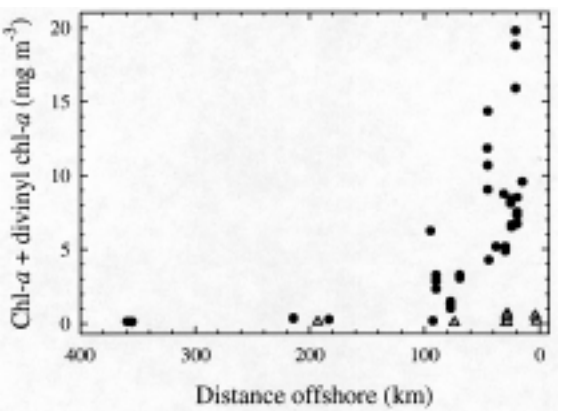

Fig. 3: Total concentration of chl-*a* (chl-*a* + divinyl chl-*a*) for all samples collected in the surface layers (0-5 m depth), plotted against approximate distance offshore, for the MIRC cruise (circles) and the Coquimbo-Iquique cruise (triangles).

Concentración total de chl-*a* (chl-*a* + divinil chl-*a*) para todas las muestras recolectadas en las capas superficiales (0-5 m de profundidad), graficada en función de la distancia aproximada costa afuera, para el crucero MIRC (círculos) y el crucero Coquimbo-Iquique (triángulos).

al. 1994, Thomas, 1999). In contrast, surface pigment concentrations were much lower for the Coquimbo-Iquique cruise (maximum 0.6 mg chl-a m^{-3}), partly because sampling did not take place within the upwelling plumes (see Fig. 1B). The highest chlorophyll concentrations were confined to a few kilometres from the coast.

The composition of accessory pigments from the surface sample (0 m) of each station, expressed as a percentage of total accessory pigments by weight, has been plotted in Fig. 4 for both cruises. Stations have been arranged according to their approximate distance from the shore. Pigment composition in the near-shore regions was characterised by a high

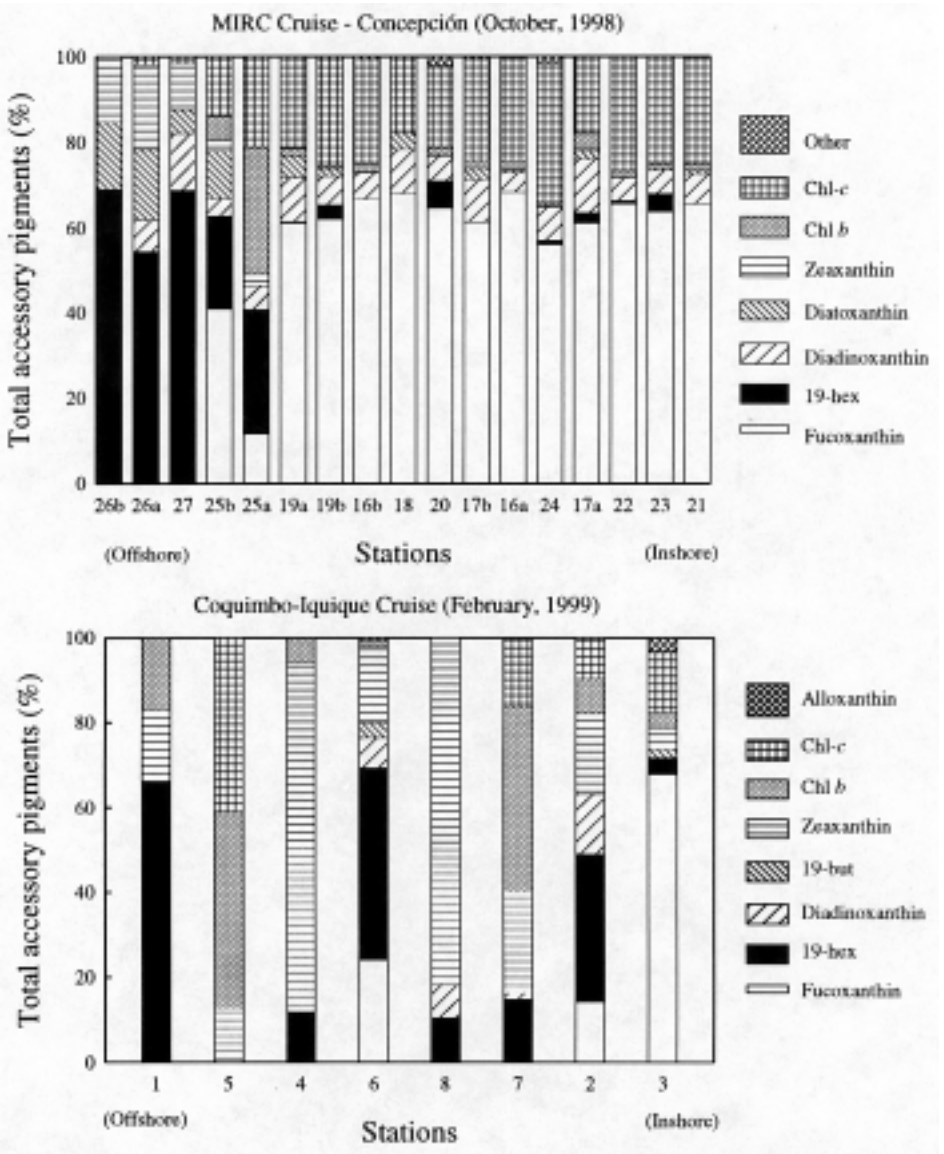

Fig. 4: Relative composition of various accessory pigments (expressed as a percentage of total accessory pigments, by weight) for surface samples (0 m) from each station. Stations have been arranged according to their distance from the coast. (A) Samples from the spring MIRC cruise, and (B) samples from the summer Coquimbo-Iquique cruise. Note: legends for the two cruises differ slightly.

Composición relativa de varios pigmentos accesorios (expresado como porcentaje del total del pigmentos accesorios, en peso) de las muestras superficiales (0 m) en cada estación. Las estaciones han sido ordenadas de acuerdo a la distancia de la costa. (A) Muestras del crucero MIRC en primavera y (B) muestras del crucero Coquimbo-Iquique en verano. Nota: las leyendas para los dos cruceros difieren levemente.

proportion of fucoxanthin and chl-c_{1+2}, indicating the presence of diatoms, typical of upwelling systems. In the MIRC cruise (spring), the diatom-dominated populations extended from the coast out to Station 19a, a distance of approximately 90 km offshore, whereas in the Coquimbo–Iquique cruise (summer), diatoms were prevalent only at Station 3, approximately 4 km from the coast. Our satellite composite image of chl-*a* concentration for the MIRC cruise (period 16-27 October, 1998) indicated a filament of elevated pigment concentration extending from the coast, north of Concepción, and descending to encompass Station 25b (see also Montecino et al. 2002). This station had a higher proportion of diatoms (high fucoxanthin/chl-*a* ratio) than the stations on either side (Fig. 4) confirming the inshore origin of this water mass. Thomas (1999) also documented the presence of these filaments in CZCS composites of pigment concentration along the Chilean coast, and noted that they originated in upwelling regions at the coast, and extended offshore over distances of approximately 300 km.

Further offshore, the MIRC cruise was characterised by phytoplankton populations with a high proportion of 19'-hexanoyloxyfucoxanthin, indicative of prymnesiophytes. The oligotrophic offshore stations (26a, 26b and 27) also contained relatively high proportions of zeaxanthin, consistent with the presence of cyanophytes. Both *Synechococcus* sp. and *Prochlorococcus* sp. contain zeaxanthin (Jeffrey & Vesk 1997), but since no divinyl chl-*a* or -*b* was recorded in the surface waters (indicative of *Prochlorococcus* sp.), this suggests that the zeaxanthin was associated with *Synechococcus* sp. All samples from the Coquimbo-Iquique cruise also contained zeaxanthin, sometimes in very high proportions. Since the surface waters of stations 4 and 5 also contained relatively high proportions of divinyl chl-*a* and divinyl chl-*b* (19-38 % of total chl-*a* or -*b*, data not shown), these waters likely contained a mixed phytoplankton assemblage consisting of *Prochlorococcus* sp., *Synechococcus* sp. and prymnesiophytes (containing 19'-hexanoyloxyfucoxanthin). A high proportion of divinyl chl-*a* and divinyl chl-*b* (4-48 % of total chl-*a* or -*b*) was also recorded at depths of 40 - 50 m for Stations 7 and 8, indicating an abundance of *Prochlorococcus* sp. at depth.

Pigment composition with depth

Vertical pigment profiles for representative inshore (Station 21) and offshore stations (Station 27) of the MIRC cruise, as well as for Station 7 from the Coquimbo-Iquique cruise, are shown in Fig. 5 (see Fig. 1 for location of sampling stations). Chl-*a* concentration was relatively uniform with depth in the top 30m for inshore Station 21, after which pigment concentration declined rapidly. At this station, the proportion of non-photosynthetic carotenoids (NPC) was relatively low, whereas the proportion of fucoxanthin/chl-*a* and chl-$c_{1,2}$/chl-*a* was high throughout the water column, indicating a predominance of diatoms at all depths. We have assumed that zeaxanthin, alloxanthin, ß-carotene, diadinoxanthin and diatoxanthin are non-photosynthetic carotenoids (NPC), and that fucoxanthin, peridinin, 19'-butanoyloxyfucoxanthin, 19'-hexanoyloxyfucoxanthin, prasinoxanthin and a-carotene are photosynthetic carotenoids, as in Bricaud et al. (1995).

In contrast, further offshore (Station 27), very low chl-*a* concentrations (~ 0.1 mg m^{-3}) were found throughout the water column, typical of the oligotrophic open ocean. Phytoplankton populations were dominated by prymnesiophytes (containing 19'-hexanoyloxyfucoxanthin and diadinoxanthin) as well as a population of cyanophytes around 30 m (containing zeaxanthin). A small percentage of divinyl chl-*a* (5-8 % of total chl-*a*) was recorded at all depths (apart from the surface sample) suggesting the presence of low numbers of *Prochlorococcus* sp. A very high proportion of NPC (mainly diadinoxanthin and zeaxanthin) was also evident down to a depth of 30 meters. Non-photosynthetic carotenoids are known to play a photoprotective role in the cell, preventing photo-oxidation at high light intensities, which are often encountered in the surface layers of oligotrophic waters (Bidigare et al. 1990). Several studies have shown that a significant portion of the vertical change in the chlorophyll-specific absorption coefficients may be attributed to the relative concentration of these photoprotective pigments (Sosik & Mitchell 1995, Babin et al. 1996, Culver & Perry 1999).

For Station 7 from the Coquimbo-Iquique cruise, vertical profiles of chl-*a* were similar to that of Station 27 from the MIRC cruise. Station 7 also displayed a high relative proportion of NPC (mainly zeaxanthin) in the surface layers indicating an abundance of cyanophytes (no divinyl chl-*a* was recorded in the surface layers). A high relative proportion of chl-*b* was also noted at this station, which increased with depth (note that chl-*b* refers to mono- and divinyl chl-*b*). In the top 30 m, the chl-*b* was most likely associated with chlorophytes, but in the

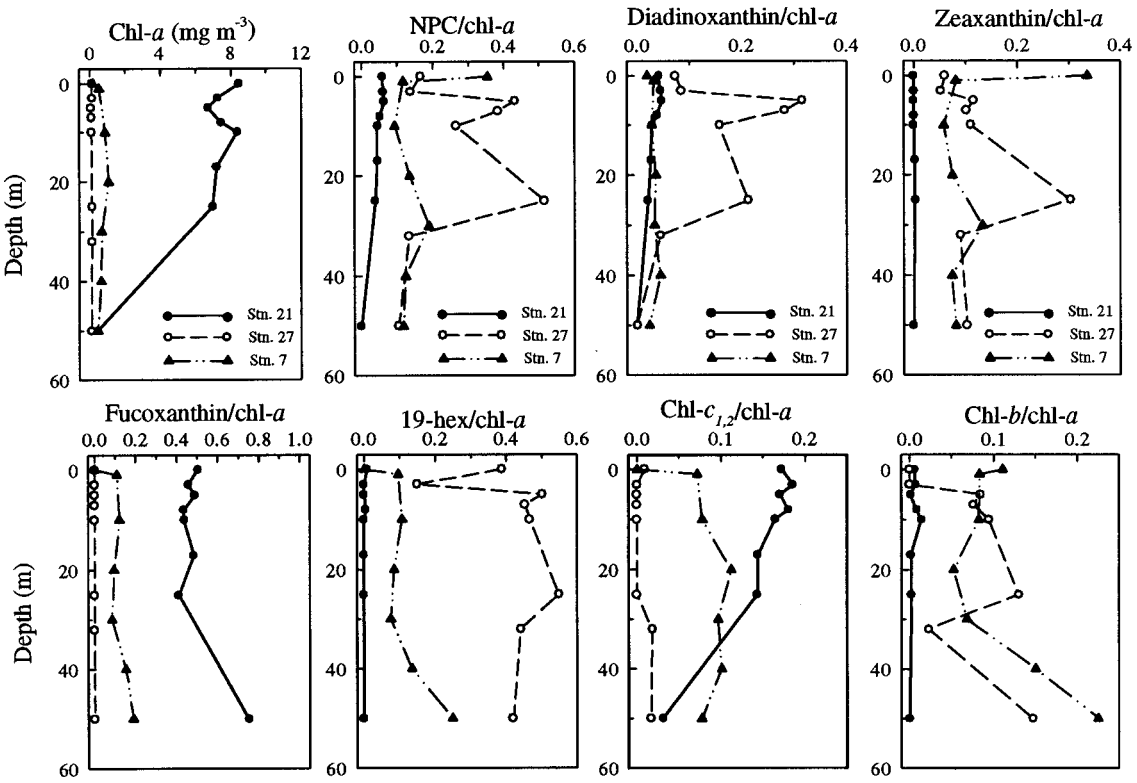

Fig. 5: Pigment profiles for an inshore station (Station 21) and an offshore station (Station 27) from the MIRC cruise, as well as Station 7 from the Coquimbo-Iquique cruise. Profiles are given for total chl-*a* (chl-*a* + divinyl chl-*a*), as well as the ratios of the following pigments, relative to chl-*a*: non-photosynthetic carotenoids (NPC), diadinoxanthin, zeaxanthin, fucoxanthin, 19'-hexanoyloxyfucoxanthin, chl-$c_{1,2}$, and total chl-*b* (chl-*b* + divinyl chl-*b*). Note: legend for top row of figures also applies to bottom row of figures.

Perfiles de pigmentos para una estación costera (Estación 21) y para una estación costa afuera (estación 27) del crucero MIRC, como también para la Estación 7 del crucero Coquimbo-Iquique. Los perfiles están dados para chl-*a* total (chl-*a* + divinil chl-*a*), así como para la razón entre los siguientes pigmentos, relativos a chl-*a*: carotenoides no-fotosintéticos (NPC), diadinoxantina, zeaxantina, fucoxantina, 19'-hexanoiloxifucoxantina, y chl-*b* total (chl-*b* + divinil chl-*b*). Nota: la leyenda de la fila superior de las figuras se aplica también a la fila inferior de las figuras.

deeper layers, where high concentrations of divinyl chl-*b* were recorded, *Prochlorococcus* sp. would predominate.

Spectral absorption characteristics

Spectral absorption properties of phytoplankton from selected depths from inshore Station 21 and offshore Station 27 of the spring MIRC cruise are shown in Fig. 6. Phytoplankton absorption characteristics are known to vary as a consequence of the composition of pigments, as well as the pigment packaging (or flattening) effect. Pigment packaging refers to the decreased absorption of pigments in cells compared with the absorption potential for the same amount of pigment in solution (Duysens 1956, Platt & Jassby 1976, Morel & Bricaud 1981, Sathyendranath et al. 1987). An increase in pigment packaging occurs either as cell size increases (e.g., for large diatom cells) or as the internal concentration of pigments increases, frequently caused by photoadaptive responses (Morel & Bricaud 1981, Kirk 1994).

For Station 21, absorption coefficients decreased markedly with depth as a result of decreasing chl-*a* concentrations (Fig. 6A), but this trend was not as noticeable in the oligotrophic offshore waters (Station 27) where pigment concentrations were relatively uniform with depth (see also Fig. 5). Phytoplankton specific absorption coefficients were substantially higher for offshore Station 27 than for Station 21, as expected for samples

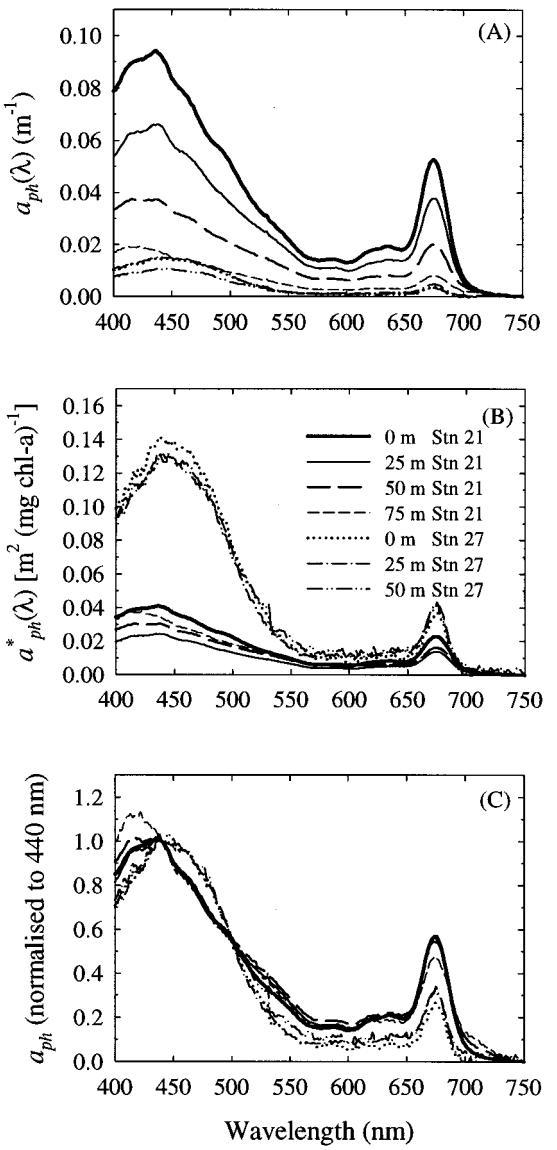

Fig. 6: Phytoplankton spectral absorption coefficients at four depths (0, 25, 50 and 75 m) for inshore Station 21 and three depths (0, 25 and 50 m) for offshore Station 27, from the MIRC cruise: (A) phytoplankton absorption m^{-1} take bercle to previene live, (B) specific phytoplankton absorption coefficients (m^2 (mg chl-*a*)$^{-1}$), and (C) phytoplankton absorption normalised to absorption at 440 nm (dimensionless). Note: legend for Fig. 6B applies to all three graphs.

Coeficientes de absorción espectral del fitoplancton a cuatro profundidades (0, 25, 50 y 75 m) para la estación 21 costera y tres profundidades (0, 25 y 50 m) para estación 27 costa afuera, del crucero MIRC: (A) absorción del fitoplancton m^{-1}, (B) coeficientes específicos de absorción del fitoplancton (m^2 (mg chl-*a*)$^{-1}$) y (C) absorción del fitoplancton normalizado por absorción a 440 nm (adimensional). Nota: la leyenda para la Fig. 6B aplica a los tres gráficos.

characterised by smaller phytoplankton species with low pigment packaging effects.

To examine differences in the spectral shape of the absorption coefficients, the absorption spectra were normalised to the absorption coefficient of phytoplankton at 440 nm (Fig. 6C). Samples from Station 27 exhibit a pronounced shouldering of absorption in the 450-480 nm region, corresponding to absorption by carotenoids (predominantly zeaxanthin). For this station, the blue absorption maximum is also shifted towards longer wavelengths, consistent with the presence of divinyl chl-*a* associated with *Prochlorococcus* sp. In contrast, the absorption maximum for the deepest sample at Station 21 (75 m) was shifted towards the shorter wavelengths, which may be attributed to absorption by phaeopigments, which increased with depth relative to chl-a concentration.

Absorption coefficients

The relationship between phytoplankton absorption at 443 nm and pigment concentration (chl-*a* + divinyl chl-*a*) is shown in Fig. 7. For the MIRC cruise, diatom-dominated samples have been separated from samples dominated by "other" phytoplankton species (predominantly prymnesiophytes and chlorophytes) by assuming that samples with a fucoxanthin/chl-*a* ratio greater than 0.35 are composed predominantly of diatoms (see inset). This separation appeared to work well, when compared with separations based on a more complete analysis of HPLC pigment composition for each sample. Diatom-dominated samples covered a wide range of chl-*a* concentrations, from 0.13-19.72 mg m^{-3} while the "other" (smaller) phytoplankton species were generally confined to the oligotrophic offshore waters, covering the range 0.07–0.20 mg chl-*a* m^{-3}.

Absorption characteristics of the "other" cells from the MIRC cruise were very similar to samples from the Coquimbo-Iquique cruise (see Fig. 7 inset), suggesting that both phytoplankton populations had similar optical properties, and were composed of cells of similar sizes. However, absorption by phytoplankton from the Coquimbo-Iquique cruise was much higher per unit chl-*a* than for the diatom-dominated samples from the MIRC cruise. For comparison, we have also included results for diatom samples collected in the Labrador Sea (data from Stuart et al. 2000). These samples had lower absorption coefficients than the diatoms from the MIRC

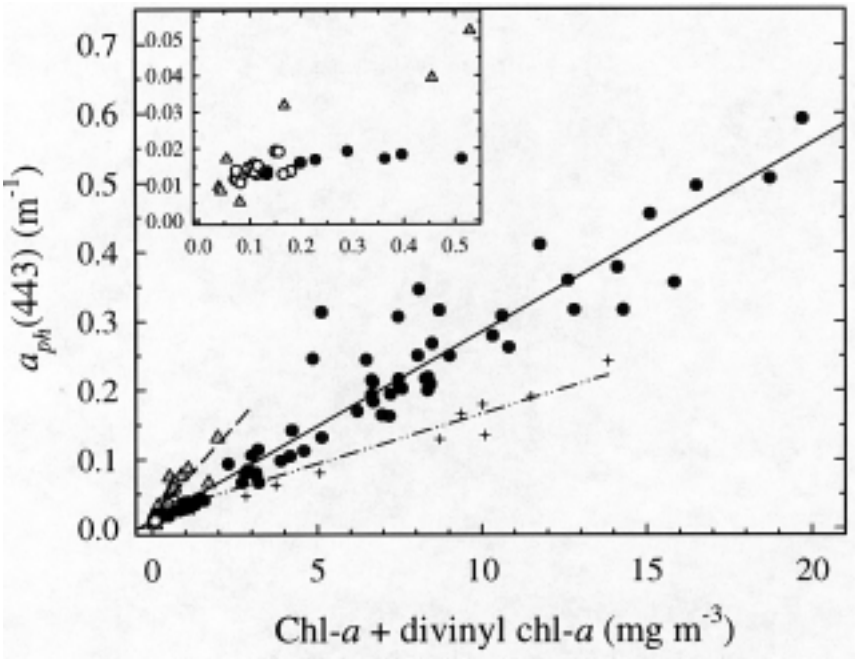

Fig. 7: Absorption coefficient of phytoplankton at 443 nm as a function of total chl-*a* concentration (chl-*a* + divinyl chl-*a*) for the MIRC cruise (diatoms = solid circles; "other" phytoplankton = open circles) and the Coquimbo-Iquique cruise (triangles, dashed line). Inset shows enlargement of the area corresponding to chl-*a* concentrations < 0.5 mg m^{-3}. Data for diatoms from the Labrador Sea (from Stuart et al. 2000) are also shown for comparison (crosses, dot-dash line). Linear regression equation for Chile diatoms (solid line): Y = 0.011 + 0.027 X (r^2 = 0.92, n = 73); equation for Coquimbo-Iquique cruise (dashed line): Y = 0.018 + 0.053 X (r^2 = 0.78, n = 13); equation for Labrador Sea diatoms: Y = 0.021 + 0.014 X (r^2 = 0.95, n = 12).

Coeficiente de absorción del fitoplancton a 443 nm en función de la concentración total de chl-*a* (chl-*a* + divinil chl-*a)* para el crucero MIRC (diatomeas = círculos rellenos; "otro" fitoplancton = círculos abiertos) y para el crucero Coquimbo-Iquique (triángulos, línea discontinua). El inserto muestra una ampliación del área correspondiente a concentraciones de chl-*a* < 0,5 mg m^{-3}. También se muestran datos para diatomeas del Mar de Labrador (de Stuart et al., 2000) como comparación (cruces, línea de puntos discontinuos). Ecuación de regresión lineal para diatomeas de Chile (línea sólida): Y = 0,011 + 0,027 X (r^2 = 0,92; n = 73); ecuación para el crucero Coquimbo-Iquique (línea discontinua): Y = 0,018 + 0,053 X (r^2 = 0,78; n = 1); ecuación para diatomeas del Mar de Labrador: Y = 0,021 + 0,014 X (r^2 = 0,95; n = 12).

cruise, the trend being most apparent at higher chlorophyll concentrations (> 5 mg m^{-3}).

Next, we examine variations in chlorophyll-specific absorption coefficients at four different wavebands, selected to correspond to those used in the SeaWiFS ocean chlorophyll (OC4) algorithm (O'Reilly et al. 1998). Phytoplankton specific absorption coefficients for samples from the MIRC cruise are shown Fig. 8 together with the relationship for a 'global' data set taken from Bricaud et al. (1995) (indicated with a dashed line). Variations in $a^*_{ph}(\lambda)$ in our study follow similar trends to those observed by Bricaud et al. (1995), although specific absorption coefficients in oligotrophic waters appear somewhat higher. It is noteworthy that Bricaud et al. (1995) also recorded a wide variation in the magnitude of $a^*_{ph}(\lambda)$ at low ambient chlorophyll concentrations, especially in the blue part of the spectrum, which they attributed fluctuations in pigment composition (mainly photoprotective carotenoids). This global data set effectively encompasses the range of observations recorded in the present study.

As expected, the diatom populations from the coastal upwelling zones have absorption characteristics that are very different from those of the mixed phytoplankton assemblages found in the oligotrophic offshore waters. At all wavelengths, the diatom-dominated populations displayed a lower $a^*_{ph}(\lambda)$ (due to a greater pigment packaging effect) than the "other" cells, with the differences being least obvious at 555 nm. There was also a clear trend of

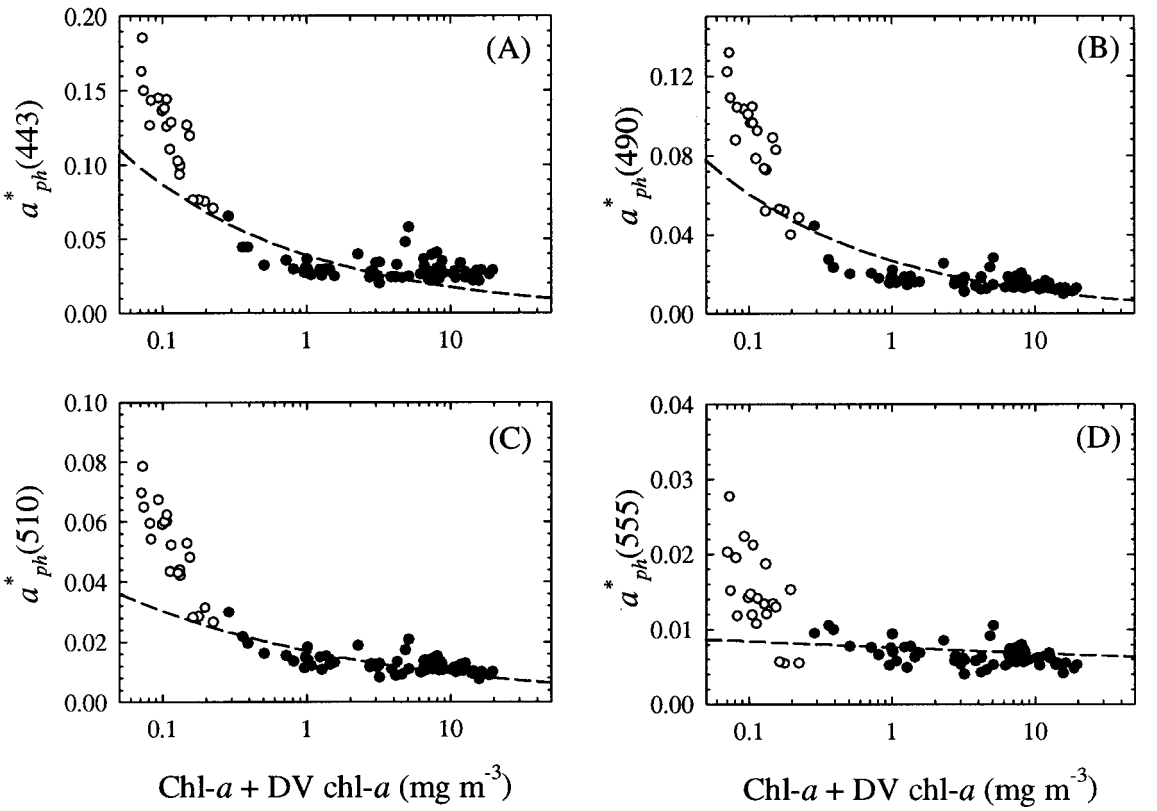

Fig. 8: Chlorophyll-specific absorption coefficients (m^2 (mg chl-*a*)$^{-1}$) of phytoplankton from the MIRC cruise at various SeaWiFS wavebands (443, 490, 510 and 555 nm) as a function of total chl-*a* concentration (chl-*a* + divinyl chl-*a*). Diatoms = solid circles (fucoxanthin/chl-*a* > 0,35; see text for details); "other" phytoplankton = open circles. Dashed line represents the relationship documented by Bricaud et al (1995) for a 'global' data set.

Coeficientes clorofila-específicos de absorción (m^2 (mg chl-*a*)$^{-1}$) de fitoplancton del crucero MIRC para varias longitudes de onda SeaWiFS (443, 490, 510 y 55 nm) como una función de la concentración de chl-*a* total (chl-*a* + divini chl-*a*). Diatomeas = círculos sólidos (fucoxantina/chl-*a* > 0,35; ver texto para más detalles); "otro" fitoplancton = círculos abiertos. La línea punteada representa la relación documentada por Bricaud et al. (1995) para un conjunto de datos "globales".

decreasing $a^*_{ph}(\lambda)$ with increasing chlorophyll concentration, as has been observed by Bricaud et al. (1995) and Sathyendranath et al. (1996). Specific absorption coefficients at 443 nm are somewhat higher than those reported by Montecino et al. (2002) for the same region although their data were normalised to the sum of fluorometrically-determined chl-*a* plus phaeopigments.

The relationship between various SeaWiFS blue/green band ratios and the relative proportion of accessory pigments is shown in Fig. 9. Linear regression analysis indicated that up to 71 % of the variance in the ratio $a_{ph}(490)/a_{ph}(555)$ could be explained by the proportion of 19'-hexanoyloxyfucoxanthin/chl-*a* (Fig. 9a; Y = 2.5 + 9.76X) and for bands $a_{ph}(443)/a_{ph}(555)$ this was reduced to 61 % (data not shown). Similarly, the proportion of fucoxanthin/chl-*a* could explain up to 67 % of the variance in the ratio $a_{ph}(490)/a_{ph}(555)$ (Fig. 9B, Y = 6.19–6.84X) and 59 % of the variance in the ratio $a_{ph}(443)/a_{ph}(555)$ (data not shown). Lower blue/green ratios are thus associated with high fucoxanthin/chl-*a* ratios (indicative of diatoms), whereas higher blue/green ratios are related to high 19'-hexanoyloxyfucoxanthin/chl-*a* ratios (indicative of prymnesiophytes). In addition, high blue/green ratios were associated with high zeaxanthin/chl-*a* ratios (indicative of cyanophytes), and in some cases, with a high relative proportion of chl-*b* (data not shown). Variation in phytoplankton absorption properties may thus be related to differences in taxonomic composition, with concomitant changes in pigment composition.

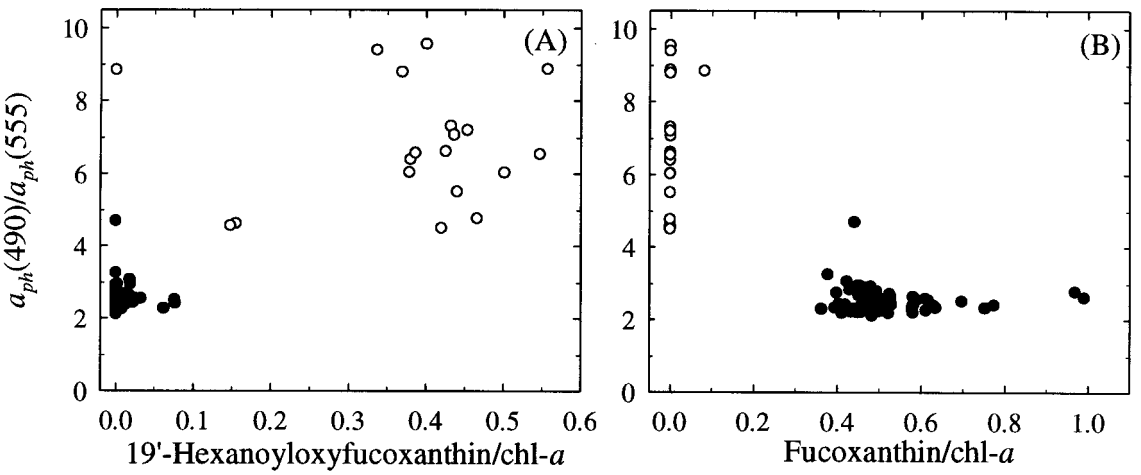

Fig. 9: (A) Ratio of phytoplankton absorption at 490 nm relative to 555 nm as a function of the ratio of 19'-hexanoyloxyfucoxanthin concentration relative to total chl-*a*. (B) Ratio of phytoplankton absorption at 490 nm relative to 555 nm as a function of the ratio of the concentration of fucoxanthin relative to total chl-*a*. All data from the MIRC cruise. Diatoms = solid circles, "other" phytoplankton = open circles.

(A) Razón de absorción de fitoplancton a 490 nm relativo a 555 nm como función de la razón de la concentración de 19'-hexanoiloxifucoxantina relativa a chl-*a* total. (B) Razón de absorción fitoplanctónica a 490 nm relativa a 555 nm como función de la concentración de fucoxantina relativa a la chl-*a* total. Todos los datos del crucero MIRC. Diatomeas = círculos sólidos, "otro" fitoplancton = círculos abiertos.

Several studies have found that pigment composition, in particular the relative proportion of non-photosynthetic carotenoids (NPC's), can account for much of the variability in phytoplankton absorption coefficients (Sosik & Mitchell 1995). In our study, the relative proportion of NPC could account for up to 59 % of the variation in the specific absorption coefficient of phytoplankton at 443 nm (Fig. 10A). Diatom-dominated samples were clearly separated from the "other" samples in this plot, and were characterised by relatively low NPC/chl-*a* ratios, with correspondingly low specific absorption coefficients. This is in direct contrast to the high specific absorption coefficients of the "other" smaller phytoplankton species, which exhibit a high relative proportion of photoprotective (i.e., non-photosynthetic) pigments.

Similarly, $a^*_{ph}(443)$ is strongly influenced by the ratio of the peak height of the Gaussian band in the blue region of the spectrum, centred at 435 nm, $p(435)$, to the peak height in the red region of the spectrum centred at 676 nm, $p(676)$ (Fig. 10B). Data for diatoms from the Labrador Sea (Stuart et al. 2000) are also indicated on this plot. Relative changes in this blue/red ratio (both associated with absorption by chl-*a*) can be related to the pigment packaging effect. From a theoretical point of view, packaging effects are greatest in spectral regions with high absorption (i.e. in the blue region of the spectrum) and less pronounced at the absorption minima (Duysens 1956, Kirk 1994). Relative changes in the ratio of $p(435)/p(676)$ can therefore be used to give some indication of the importance of the packaging effect, since the red absorption peak is less affected by pigment packaging by virtue of its smaller magnitude.

Blue/red ratios were lowest for diatom-dominated samples and highest for the other samples (comprised of smaller cells), suggesting that packaging of pigments is strongly related to cell size. It is noteworthy that many of the diatom samples from the Labrador Sea had lower $p(435)/p(676)$ ratios than diatoms from Chile, implying a greater flattening effect (and perhaps larger cell size). A strong, linear relationship was obtained between $a^*_{ph}(443)$ and the ratio of peak height in the blue to that in the red part of the spectrum for all data combined ($a^*_{ph}(443) = -0.075 + 0.065 * p(435)/p(676)$, $r^2=0.88$), implying that the packaging effect plays a major role in modifying phytoplankton absorption, accounting for up to 88% of the total variation in specific absorption coefficients in these samples. In fact, multiple

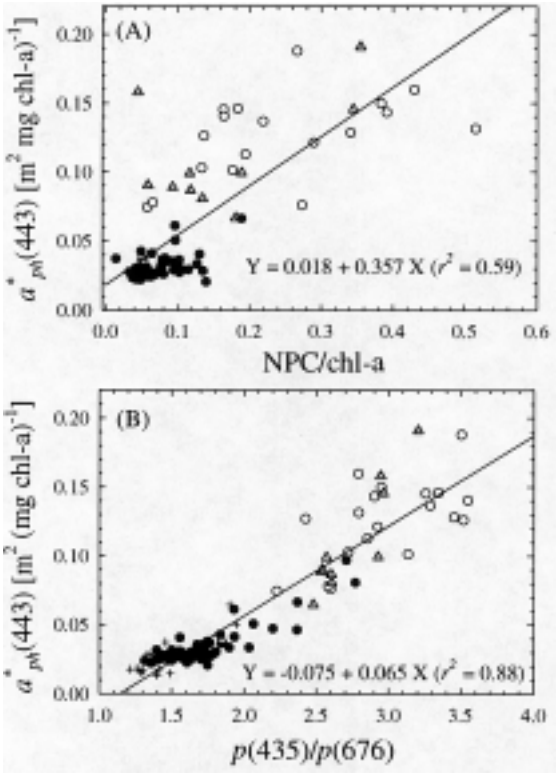

Fig. 10: (A) Chlorophyll-specific absorption coefficient of phytoplankton at 443 nm as a function of the ratio of non-photosynthetic carotenoids (NPC) to chl-*a*, for the MIRC cruise (diatoms = solid circles, "other" phytoplankton = open circles) and the Coquimbo-Iquique cruise (triangles). (B) Chlorophyll-specific absorption coefficient of phytoplankton at 443 nm as a function of the ratio of the Gaussian peak height in the blue, *p*(435), to that in the red region of the spectrum, *p*(676), for the MIRC cruise (diatoms = solid circles, "other" phytoplankton = open circles), the Coquimbo-Iquique cruise (triangles) and diatoms from the Labrador Sea (crosses, data from Stuart et al. 2000).

Coeficientes clorofila-específicos del fitoplancton a 443 nm en función de la razón de carotenoides no-fotosintéticos (NPC) a chl-*a*, para el crucero MIRC (diatomeas = círculos sólidos, "otro" fitoplancton = círculos abiertos) y crucero Coquimbo-Iquique (triángulos). (B) Coeficientes clorofila-específicos del fitoplancton a 443 nm en función de la razón de la altura del pico Gaussiano en el azul, *p*(435), al de la región del rojo del espectro, *p*(676), para el crucero MIRC (diatomeas = círculos sólidos, "otro" fitoplancton = círculos abiertos), el crucero Coquimbo-Iquique (triángulos) y diatomeas del Mar de Labrador (cruces, datos de Stuart et al. 2000).

linear regression analysis revealed that NPC/chl-*a* and *p*(435)/*p*(676) together could account for up to 92 % of the total variation in $a^*_{ph}(443)$ for the MIRC cruise. Since samples dominated by diatoms are clearly separated from the other samples in Fig. 10b, plots such as these can be used to reveal differences in optical properties of phytoplankton from different geographic regions, which would in turn reflect differences in phytoplankton community structure.

Comparison with satellite-derived chl-a

To test whether the variability in optical characteristics of phytoplankton observed during this study affects the reliability of routine algorithms used for remote sensing of chl-*a*, we compared in situ estimates of chl-*a* (fluorometric and HPLC) with satellite-derived estimates, for the MIRC cruise. Samples collected from the surface layers (0 m) at each station were used for in situ chl-*a* estimates, and satellite values of chl-*a* were computed only for cloud-free stations. For the satellite-derived estimates of chl-*a*, each data point represents a mean of 9 pixels (3 x 3 matrix) around the central value. See Table 1 for the mean satellite chlorophyll concentrations (± SD) for the cloud-free stations, as well as the time difference between the satellite overpass and the time of in situ sampling.

At low in situ chl-*a* concentrations (< 0.4 mg m^{-3}), the satellite-derived estimates of chl-*a* were somewhat higher than those obtained through HPLC analysis (Fig. 11A), which may be related to the high phytoplankton specific absorption coefficients observed at low chlorophyll concentrations (see Fig. 8). Satellite-derived values of chl-*a* compared reasonably well with in situ fluorometric estimates (Fig. 11B), with the slope of the line being close to one. The absolute percent difference between satellite and ship chl-*a* was less for fluorometric chl-*a* (42.89 ± 33.21 %) than for HPLC chl-*a* data (61.44 ± 56.93 %). It should also be borne in mind that there are often systematic differences between HPLC and fluorometric determinations of chl-*a*, with fluorometric estimates often overestimating total chl-*a* concentration. For example, if divinyl chl-*a* (usually present at low pigment concentrations) were not resolved into monovinyl and divinyl chl-*a* (as in the case of fluorometric determinations) this could result in a 10-15 % overestimation of total chl-*a* concentration (see Latasa et al. 1996). Furthermore, high concentrations of chl-*c*, frequently associated with diatoms, have been shown to cause overestimates in the concentration of chl-*a* when measured fluorometrically (Lorenzen 1981, Bianchi et al. 1995). It is interesting to note that the SeaWiFS OC4v4 algorithm is derived from the new SeaBAM data set, which is heavily biased towards fluorometric pigment determinations. Only 28 % of the 2,853 in situ chl-*a* determinations used to develop the OC4v4 algorithm were derived by HPLC analysis, whereas 72 % were from fluorometric measurements (O'Reilly et al. 2000). It is therefore not surprising that there was a closer agreement between satellite and in situ fluorometric chl-*a* (Fig. 11B), than between satellite and HPLC chl-a measurements (Fig. 11A).

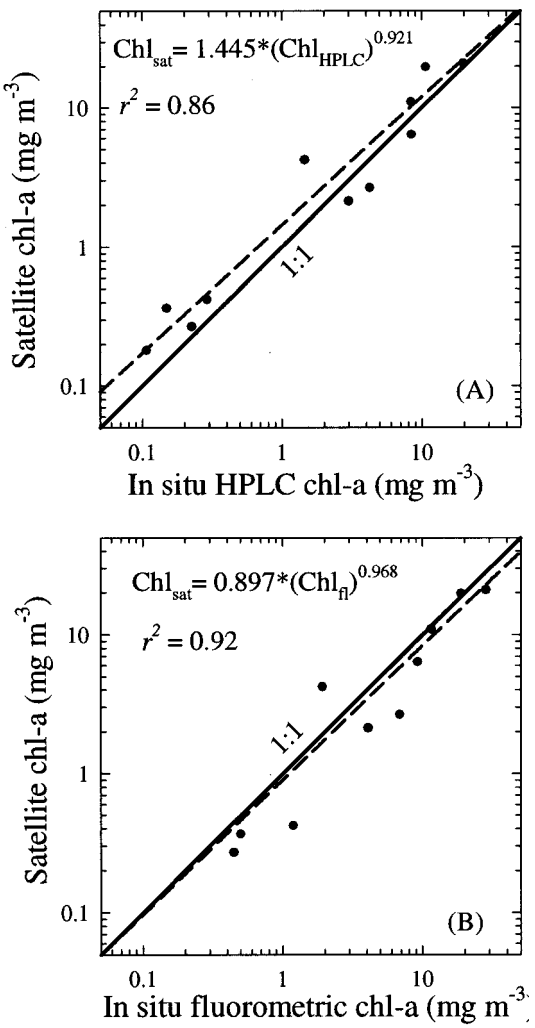

Fig. 11: (A) Comparison between satellite-derived chl-*a* (see text for details) and in situ HPLC-derived total chl-*a* for the spring MIRC cruise. (B) Comparison between satellite-derived chl-*a* and in situ fluorometric chl-*a*, for the spring MIRC cruise.

(A) Comparación entre la chl-*a* derivada del satélite (ver el texto para los detalles) y chl-*a* total in situ derivada por HPLC para el crucero MIRC de primavera. (B) Comparación entre chl-*a* derivada del satélite y chl-*a* fluorométrica *in situ*, para el crucero MIRC de primavera.

DISCUSSION

Pigment distribution and composition

The patterns in chl-*a* distribution observed during the two cruises are characteristic of that found in upwelling regions. Upwelling brings nutrient-rich water to the surface in the inshore region, which in turn fuels an increase in phytoplankton biomass and primary production (Barber & Smith 1981, Thomas et al. 1994, Strub et al. 1998). Typically, off the coast of Chile, the surface phytoplankton concentrations are high over the shelf break, frequently exceeding 10 mg chl m^{-3}, with lower pigment concentrations over the mid-shelf and offshore regions (Morales et al. 1996, 2001). CZCS satellite images have been used by Thomas et al. (2001) to document seasonal variations in phytoplankton pigment concentrations off the coast of Chile. Generally, high inshore pigment concentrations were noted throughout the year south of 33º S, whereas further north, the near-

coast pigment concentrations were much lower, with pigment concentrations > 1.0 mg chl-*a* m^{-3} found only within 10 km of the coast. This is consistent with the pigment distribution patterns observed during the two cruises in this study. It should also be noted that the continental shelf off the coast of Chile is often extremely narrow, practically non-existent in some areas, which could also help to account for the lower pigment concentrations encountered along the northern coast of Chile (i.e., Coquimbo-Iquique cruise).

Variations in phytoplankton pigment composition were used to infer taxonomic groupings; large differences in phytoplankton species composition were observed within cruises as well as between cruises (see Fig. 4). High concentrations of diatoms were found in the near-shore upwelling zones off the coast of Concepción during the spring cruise, but concentrations were much lower during the summer Coquimbo-Iquique cruise. Seasonal shifts in diatom abundance may be implicated, since diatoms are typical of spring blooms. Differences in latitude and climatic conditions may further contribute to differences between the two sampling regions, but it is not possible to interpret seasonal trends in a more rigorous fashion with such a limited data set. Phytoplankton populations in the oligotrophic offshore zones were dominated by smaller species such as prymnesiophytes, chlorophytes, cyanophytes and *Prochlorococcus* sp. Similarly, Morales et al. (1996, 2001) noted that in northern Chile, smaller cells dominated samples with relatively low chlorophyll concentrations, whereas high chlorophyll concentrations were predominantly associated with larger net phytoplankton (> 20 mm).

There was also some evidence of photoacclimation in samples from oligotrophic stations (Stations 7 and 27). A notable increase in the relative proportion of photoprotective pigments was found in the top 10 m (diadinoxanthin for Station 27, and zeaxanthin for Station 7), as well as an increase in chl-*b*/chl-*a* ratio with depth. Furthermore, the NPC/chl-*a* ratio was substantially higher at the oligotrophic stations than for stations from the eutrophic inshore waters (e.g., Station 21). Phytoplankton adapt to changes in light intensity with depth both by increasing their intracellular pigment content, and by changing the ratio of accessory pigments. High concentrations of photoprotective pigments are a characteristic feature of oligotrophic waters (Bricaud et al. 1995, Stuart et al. 1998), and can also be related to cell size. At high irradiances (typically in the top 20 m in clear oceanic waters), phytoplankton photosynthesis becomes photoinhibited because of damage to proteins of the photosystem by UV wavelengths. Phytoplankton cells counteract these detrimental effects by increasing the amount of photoprotective pigments (e.g., zeaxanthin), which absorb light but do not pass it on to Photosystem II. Smaller phytoplankton cells, with larger surface area/volume ratios, sustain greater amounts of damage (induced by UV exposure) per unit of DNA, than larger cells (Karentz et al., 1991). Conversely, larger diatom species are relatively resistant to UV-radiation (Helbling et al. 1994), which would explain the low NPC/chl-*a* ratios from the eutrophic inshore region.

Furthermore, an increase in the relative proportion of chl-*b* with depth would enable more efficient collection of photons in the blue part of the spectrum, the wavelengths which are least attenuated with depth (Moore et al. 1995). *Prochlorococcus* sp. are known to undergo dramatic changes in the ratio of chl-*b*/chl-*a* with depth, (Goericke & Repeta 1993), although in some cases this was also related to changing populations with depth.

Absorption characteristics

Diatoms could be effectively separated from "other" phytoplankton species in the MIRC cruise using their high fucoxanthin/chl-*a* ratio (> 0.35). This allowed for a comparison of the absorption characteristics of the different phytoplankton groups. In a similar fashion, Stuart et al. (2000) used the ratio of chl-c_3/chl-*a* successfully to separate prymnesiophytes in the Labrador Sea from other phytoplankton species. Spectral absorption characteristics of the inshore diatom population and offshore mixed phytoplankton assemblage showed different trends, with the offshore population exhibiting a red-shift in the blue absorption maximum, associated with absorption by divinyl chl-*a*, as well as a shoulder around 480 nm, attributed to absorption by zeaxanthin.

Offshore populations exhibited much higher phytoplankton specific absorption coefficients than the inshore populations. Differences in specific absorption coefficients may be attributed to two factors: changes in pigment packaging, and changes in pigment composition. Pigment packaging is known to be a function of cell size as well as intracellular pigment concentration (Duysens 1956). Lower specific absorption coefficients and greater pigment packaging effects are generally

associated with larger diatom cells, since light absorption by phytoplankton cells is scaled to their cross-sectional area (Agustí 1991). Recently, Ciotti et al. (2002) demonstrated that by specifying cell size of the dominant organism, more than 80 % of the variability in the spectral shape of the phytoplankton absorption coefficient could be explained. It is noteworthy that diatom populations from the upwelling area off the coast of Chile had higher absorption coefficients than diatom populations from the Labrador Sea (see Fig. 7). This would imply that not all diatom species have the same optical properties, despite the fact that they have a similar complement of accessory pigments. In this case, cell size and the related pigment-packaging effects, would be the major factor governing the optical properties. Absorption coefficients for the Labrador Sea diatoms, mean $a^*_{ph}(443)$ = 0.0268 m^2 (mg chl $a)^{-1}$ (Stuart et al. 2000), are consistent with those of large diatoms (> 20 mm) from Antarctic Peninsula waters (Mitchell & Holm-Hansen 1991, Brody et al. 1992). For comparison, the mean specific absorption coefficient of diatoms from this study was 0.0324 m^2 (mg chl $a)^{-1}$. Furthermore, the lower $p(435)/p(676)$ ratios recorded for the Labrador Sea diatoms (Fig. 10B) are also consistent with those of large cells with a high pigment packaging effect. Photoadaptation to the low light levels encountered in high latitude areas would result in high intracellular pigment concentrations (Arrigo et al. 1993), further enhancing the pigment-packaging effect for diatoms from the Labrador Sea.

Blue/green ratios

Algorithms based upon blue/green ratios have been used extensively to derive chlorophyll concentrations from ocean-colour data (Morel & Prieur 1977, Carder et al. 1986, Gordon et al. 1988, O'Reilly et al. 1998). These algorithms relate the ratio of remote-sensing reflectance at two wavelengths in the blue and green parts of the spectrum, to chlorophyll concentration. Since reflectance is a function of the absorption coefficient, any change in the spectral absorption coefficients of phytoplankton could potentially affect the performance of these algorithms. In this study, we demonstrate that the blue/green absorption ratios $a_{ph}(443)/a_{ph}(555)$ and $a_{ph}(490)/a_{ph}(555)$ are related to pigment composition, high ratios being associated with a high relative proportion of 19'-hexanoyloxyfucoxanthin (an indicator of prymnesiophytes) and low blue/green ratios being associated with a high relative proportion of fucoxanthin (an indicator of diatoms). The proportion of non-photosynthetic carotenoids could account for some 59 % of the total variation in specific absorption coefficients of phytoplankton at 443 nm, whereas changes in the pigment-packaging effect (associated with variations in the Gaussian peak height of chl-*a* absorption in the blue to red regions of the spectrum) could account for up to 88 % of the variation in $a^*_{ph}(443)$. Similarly, Stuart et al. (1998) noted that package effects were responsible for 58–71 % of the variability in phytoplankton absorption at 440 nm in samples collected from the Arabian Sea and Saanich Inlet (Vancouver Island). Both pigment concentration and cell size change the optical absorption cross-section through the package effect. Pigment composition, on the other hand, may play a secondary role in modifying phytoplankton absorption coefficients, especially when considering the variation in absorption coefficients of diatoms from Chile and the Labrador Sea, which have a similar pigment complement.

Comparison of satellite and in situ chl-a

Currently, blue/green algorithms for the operational retrieval of chl-*a* from remotely-sensed, ocean-colour data (e.g., SeaWiFS) are applied globally. However, numerous studies have suggested that species-specific or regional algorithms need to be developed to account for differences in bio-optical characteristics (Fenton et al. 1994, Carder et al. 1999, Gibb et al. 2000, Sathyendranath et al. 2001). The global OC4v4 algorithm appeared to perform reasonably well in the upwelling region off the coast of Chile, despite the fact that wide variations were observed in phytoplankton absorption coefficients in this study (inshore versus offshore). This may be attributed to the fact that global $a^*_{ph}(\lambda)$ vs chlorophyll relationships encompass the regional variations observed in this study. Variations in the magnitude of $a^*_{ph}(\lambda)$ have been shown to be correlated with chlorophyll concentration (Bricaud et al. 1995) and this is implicitly included in global ocean-colour ratio algorithms. However, it is the nature of a^*_{ph} versus chl-*a* relationships to vary from one region to another, and it is likely that the observed differences between satellite and in situ chl-*a* (43 % for fluorometric chl-*a* and 61 % for HPLC chl-*a*) could perhaps be reduced by using regional algorithms. Note that the SeaWiFS Project requires agreement between

the in situ and remotely sensed observations of chl-*a* to within 35 % over the range 0.05 – 50 mg m^{-3} (Hooker & Esaias 1993). This might achieved if regional algorithms were developed, but it is not the scope of this paper. The data set used to construct the SeaWiFS algorithm is heavily weighted in favour of fluorometric determinations of in situ chl-*a*, which may explain why the satellite comparison with fluorometric chl-*a* works better than with HPLC chl-*a*.

ACKNOWLEDGEMENTS

We thank Heather Bouman, César Fuentes-Yaco and two anonymous referees for their input and constructive comments on the manuscript. We are also grateful to Cathy Porter, Heidi Maass, Gabriel Yuras and Larry Gabert for processing the satellite imagery. The work presented in this paper was supported, in part, by a research grant from NSERC (Canada) and the Department of Fisheries and Oceans, Canada as well as by the Chilean National commission for Scientific and Technological Research (CONICYT) through the FONDAP Program, and by the Fundación Andes. We thank the officers, technicians and crew of the R/V *Abate Molina* for help and support at sea.

LITERATURE CITED

AGUSTÌ S (1991) Allometric scaling of light absorption and scattering by phytoplankton cells. Canadian Journal of Fisheries and Aquatic Sciences 48: 763-767.

ARRIGO KR, DH ROBINSON & CW SULLIVAN (1993) A high resolution study of the platelet ice ecosystem in McMurdo Sound, Antarctica: photosynthetic and bio-optical characteristics of a dense microalgal bloom. Marine Ecology Progress Series 98: 173-185.

BABIN M, A MOREL, H CLAUSTRE, A BRICAUD, Z KOLBER & PG FALKOWSKI (1996) Nitrogen- and irradiance-dependent variations of the maximum quantum yield of carbon fixation in eutrophic, mesotrophic and oligotrophic marine systems. Deep-Sea Research I 43: 1241-1272.

BARBER RT & RL SMITH (1981) Coastal upwelling ecosystems. In: Longhurst AR (ed) Analysis of marine ecosystems: 741. Academic Press, Toronto, Canada.

BIANCHI TS, C LAMBERT & DC BIGGS (1995) Distribution of chlorophyll *a* and phaeopigments in the northwestern Gulf of Mexico: a comparison between fluorometric and high-performance liquid chromatography measurements. Bulletin of Marine Science 56: 25-32.

BIDIGARE RR, ME ONDRUSEK, JH MORROW & DA KIEFER (1990) *In vivo* absorption properties of algal pigments. Proceedings of the Society of Photo-Optical Instrumentation Engineers, Ocean Optics X 1302: 290-302.

BRICAUD A & D STRAMSKI (1990) Spectral absorption coefficients of living phytoplankton and nonalgal biogenous matter: a comparison between the Peru upwelling area and the Sargasso Sea. Limnology and Oceanography 35: 562-582.

BRICAUD A, M BABIN, A MOREL & H CLAUSTRE (1995) Variability in the chlorophyll-specific absorption coefficients of natural phytoplankton: analysis and parameterization. Journal of Geophysical Research 100: 13,321-13,332.

BRODY E, BG MITCHELL, O HOLM-HANSEN & M VERNET (1992) Species-dependent variations of the absorption coefficient in the Gerlache Strait. Antarctic Journal of the United States 27: 160-162.

CARDER KL, RG STEWARD, JH PAUL & GA VARGO (1986) Relationships between chlorophyll and ocean color constituents as they affect remote-sensing reflectance models. Limnology and Oceanography 31: 403-413.

CARDER KL, FR CHEN, ZP LEE, SK HAWES & D KAMYKOWSKI (1999) Semianalytic Moderate-Resolution Imaging Spectrometer algorithms for chlorophyll *a* and absorption with bio-optical domains based on nitrate-depletion temperatures. Journal of Geophysical Research 104: 5403-5421.

CULVER ME & MJ PERRY (1999) The response of photosynthetic absorption coefficients to irradiance in culture and in tidally mixed estuarine waters. Limnology and Oceanography 44: 24-36.

DUYSENS LNM (1956) The flattening of the absorption spectrum of suspensions, as compared to that of solutions. Biochimica et Biophysica Acta 19: 1-12.

FENTON N, J PRIDDLE & P TETT (1994) Regional variations in bio-optical properties of the surface waters in the Southern Ocean. Antarctic Science 6: 443-448.

GIBB SW, RG BARLOW, DG CUMMINGS, NW REES, CC TREES, P HOLLIGAN & D SUGGETT (2000) Surface phytoplankton pigment distributions in the Atlantic Ocean: an assessment of basin scale variability between 50º N and 50º S. Progress in Oceanography 45: 339-368.

GORDON HR, OB BROWN, RH EVANS, JW BROWN, RC SMITH, KS BAKER & DK CLARK (1988) A semianalytic radiance model of ocean color. Journal of Geophysical Research 93: 10,909-10,924.

HEAD EJH & EPW HORNE (1993) Pigment transformation and vertical flux in an area of convergence in the North Atlantic. Deep-Sea Research II 40: 329-346.

HOEPFFNER N & S SATHYENDRANATH (1991) Effect of pigment composition on absorption properties of phytoplankton. Marine Ecology Progress Series 73: 11-23.

HOEPFFNER N & S SATHYENDRANATH (1992) Bio-optical characteristics of coastal waters: Absorption spectra of phytoplankton and pigment distribution in the western North Atlantic. Limnology and Oceanography 37: 1660-1679.

HOEPFFNER N & S SATHYENDRANATH (1993) Determination of the major groups of phytoplankton pigments from the absorption spectra of total particulate matter. Journal of Geophysical Research 98: 22,789-22,803.

HOLM-HANSEN O, CJ LORENZEN, RW HOLMES & JDH STRICKLAND (1965) Fluorometric determination of chlorophyll. Journal du Conseil 30: 3-15.

HOOKER SB & WE ESAIAS (1993) An Overview of the SeaWiFS Project. EOS, Transactions, American Geophysical Union 74: 241-246.

JEFFREY SW & M VESK (1997) Introduction to marine phytoplankton and their pigment signatures. In: Jeffrey SW, RFC Mantoura & SW Wright (eds) Phytoplankton pigments in oceanography: 37-84. UNESCO Publishing, Paris, France.

KIRK JTO (1994) Light and photosynthesis in aquatic ecosystems. Cambridge University Press, Cambridge, United Kingdom. 509 pp.

KISHINO M, M TAKAHASHI, N OKAMI & S ICHIMURA (1985) Estimation of the spectral absorption coefficients of phytoplankton in the sea. Bulletin of Marine Science 37: 634-642.

LATASA M, RR BIDIGARE, ME ONDRUSEK & MC KENNICUTT (1996) HPLC analysis of algal pigments: a comparison exercise among laboratories and recommendations for improved analytical performance. Marine Chemistry 51: 315-324.

LORENZEN CJ (1981) Chlorophyll *b* in the eastern North Pacific Ocean. Deep-Sea Research 28A: 1049-1056.

LUTZ VA, S SATHYENDRANATH & EJH HEAD (1996) Absorption coefficient of phytoplankton: Regional variations in the North Atlantic. Marine Ecology Progress Series 135: 197-213.

MACKEY DJ, HW HIGGINS, MD MACKEY & D HOLDSWORTH (1998) Algal class abundances in the western equatorial Pacific: estimation from HPLC measurements of chloroplast pigments using CHEMTAX. Deep-Sea Research I 45: 1441-1468.

MITCHELL BG & O HOLM-HANSEN (1991) Bio-optical properties of Antarctic Peninsula waters: differentiation from temperate ocean models. Deep-Sea Research 38: 1009-1028.

MONTECINO V, R ASTORECA, G ALARCÓN, G PIZARRO, L RETAMAL & O ULLOA (2004) Bio-optical characteristics and primary productivity during up welling and non-up welling conditions in a highly productive coastal ecosystem off Chile (36º S). Deep Sea Research.

MORALES CE, JL BLANCO, M BRAUN, H REYES & N SILVA (1996) Chlorophyll-*a* distribution and associated oceanographic conditions in the upwelling region off northern Chile during the winter and spring 1993. Deep-Sea Research I 43: 267-289.

MORALES CE, JL BLANCO, M BRAUN & N SILVA (2001) Chlorophyll-*a* distribution and mesoscale physical processes in upwelling and adjacent oceanic zones off northern Chile (summer-autumn 1994). Journal of the Marine Biological Association of the United Kingdom 81: 193-206.

MOREL A & A BRICAUD (1981) Theoretical results concerning light absorption in a discrete medium, and application to specific absorption of phytoplankton. Deep-Sea Research I 28A: 1375-1393.

MOREL A & L PRIEUR (1977) Analysis of variations in ocean color. Limnology and Oceanography 22: 709-722.

O'REILLY JE, S MARITORENA, BG MITCHELL, DA SIEGEL, KL CARDER, SA GARVER, M KAHRU & C MCCLAIN (1998) Ocean color chlorophyll algorithms for SeaWiFS. Journal of Geophysical Research 103: 24,937-24,953.

O'REILLY JE, S MARITORENA, D SIEGEL, MC O'BRIEN, D TOOLE, BG MITCHELL, M KAHRU, FP CHAVEZ, P STRUTTON, G COTA, SB HOOKER, CR MCCLAIN, KL CARDER, F MÜLLER-KARGER, L HARDING, A MAGNUSON, D PHINNEY, GF MOORE, J AIKEN, KR ARRIGO, R LETELIER & M CULVER (2000) Ocean color chlorophyll a algorithms for SeaWiFS, OC2, and OC4, Version 4. In: Hooker SB ER & Firestone (eds) SeaWiFS Postlaunch Technical Report Series: SeaWiFS Postlaunch Calibration and Validation Analyses, Part 3: 9-23. NASA, Goddard Space Flight Center, Greenbelt, Maryland.

PLATT T & AD JASSBY (1976) The relationship between photosynthesis and light for natural assemblages of coastal marine phytoplankton. Journal of Phycology 12: 421-430.

RYTHER JH (1969) Photosynthesis and fish production in the sea. Science 166: 72-76.

SATHYENDRANATH S, L LAZZARA & L PRIEUR (1987) Variations in the spectral values of specific absorption of phytoplankton. Limnology and Oceanography 32: 403-415.

SATHYENDRANATH S, T PLATT, V STUART, BD IRWIN, MJW VELDHUIS, GW KRAAY & WG HARRISON (1996) Some bio-optical characteristics of phytoplankton in the N.W. Indian Ocean. Marine Ecology Progress Series 132: 299-311.

SATHYENDRANATH S, V STUART, BD IRWIN, H MAASS, G SAVIDGE, L GILPIN & T PLATT (1999) Seasonal variations in bio-optical properties of phytoplankton in the Arabian Sea. Deep-Sea Research 46: 633-654.

SATHYENDRANATH S, V STUART, G COTA, H MAASS & T PLATT (2001) Remote sensing of phytoplankton pigments: a comparison of empirical and theoretical approaches. International Journal of Remote Sensing 22: 249-273.

SOSIK HM & BG MITCHELL (1995) Light absorption by phytoplankton, photosynthetic pigments and detritus in the California Current System. Deep-Sea Research I 42: 1717-1748.

STRUB PT, JM MESIAS, V MONTECINO, J RUTLLANT & S SALINAS (1998) Coastal ocean circulation off western South America. In: Robinson AR & KH Brink (eds) The sea: 273-313. John Wiley, New York, New York, USA.

STUART V, S SATHYENDRANATH, T PLATT, H MAASS & BD IRWIN (1998) Pigments and species composition of natural phytoplankton populations: effect on the absorption spectra. Journal of Plankton Research 20: 187-217.

STUART V, S SATHYENDRANATH, EJH HEAD, T PLATT, B IRWIN & H MAASS (2000) Bio-optical characteristics of diatom and prymnesiophyte populations in the Labrador Sea. Marine Ecology Progress Series 201: 91-106.

THOMAS AC (1999) Seasonal distributions of satellite-measured phytoplankton pigment concentration along the Chilean coast. Journal of Geophysical Research 104: 25,877-25,890.

THOMAS AC, PT STRUB, F HUANG & C JAMES (1994) A comparison of the seasonal and interannual variability of phytoplankton pigment concentrations in the Peru and California current system. Journal of Geophysical Research 99: 7355-7370.

THOMAS AC, M-E CARR & PT STRUB (2001) Chlorophyll variability in eastern boundary currents. Geophysical Research Letters 28: 3421-3424.

Associate Editor: Vivian Montecino
Received October 29, 2002; accepted October 1, 2003